Small time and spatial scale variability of phytoplankton biomass on the north Norwegian shelf in 1995

Sergei Babichenko, Paul Wassmann, Larisa Poryvkina & Inger J. Andreassen

SARSIA

Babichenko S, Wassmann P, Poryvkina L, Andreassen IJ. 1999. Small time and spatial scale variability of phytoplankton biomass on the north Norwegian shelf in 1995. *Sarsia* 84:293-302.

The temporal and spatial short-term variability of phytoplankton biomass was investigated in spring, summer and autumn in a polygon crossing the north Norwegian shelf between the two coastal banks Sveinsgrunnen and Malangsgrunnen. In addition to traditional sampling (CTD, nutrients and chlorophyll *a*), a remote sensing lidar technique was used to continuously investigate the phytoplankton biomass. The number of sensing spots on each of the 6 tracks through the polygon (lasting for about 18 hours) corresponded to about 100 000 sampling procedures. The penetration depth of the lidar ranged from 15 to 30 m. High spatial and temporal short-term dynamics (1.5-2.5 nautical miles, 2 days) were recorded, apparently due to patches of phytoplankton (up to 4 times above background concentrations) observed in the study area. No strong relationship between variable water masses (as defined by temperature and salinity) and phytoplankton biomass could be established in the polygon. Care must be taken to interpret seasonal or spatial phytoplankton distribution on the north Norwegian shelf when sampling is carried out at time intervals greater than 1 day and spatial resolution more than 2 nautical miles.

Sergei Babichenko & Larisa Poryvkina, Institute of Ecology, Kevade 2, EE-0001 Tallinn, Estonia. – Paul Wassmann & Inger J. Andreassen, Norwegian College of Fishery Science, University of Tromsø, N-9037 Tromsø, Norway.
E-mail: (Babichenko & Poryvkina) ldi@anet.ee – paulw@nfh.uit.no – i-andrea@online.no

Keywords:Phytoplankton; fluorescence; remote sensing.

INTRODUCTION

Recent conceptual models of the trophodynamic functioning of planktonic ecosystems (Legendre & Le Fèvre 1989, 1995) proposed that hydrodynamic singularities, such as fronts, eddies and upwelling play a major role in favouring new production over *in situ* recycling and, as a result, the prevalence of short food webs over the microbial loop. According to these models, physical forces act upon the biological system in a series of bifurcations by setting the conditions leading to the dominance of a given microplankton assemblage and by controlling the process involved in the fate of produced matter. For example, in slope currents and across shelf-breaks, frontal structures and vertical mixing are crucial in controlling phytoplankton primary production, activity of grazers and ultimately in determining the structure of the pelagic food web in that area (e.g. Holligan & al. 1984; Kahru & al. 1984; Kiørboe & al. 1988; Fernandez & al. 1993). This implies that the extensive physical forcing on shelf is of utmost significance for their plankton dynamics, favouring new production, biomass accumulation as well as vertical and horizontal export of organic matter.

The first seasonal investigation of the hydrography, nutrients and phytoplankton dynamics on the north Norwegian shelf was carried out at Nordvestbanken in 1994 (Nordby & al. 1999). Each month one survey crossing Nordvestbanken, which lasted for about 2 days, was carried out between March and October (Ratkova & al. 1999; Wassmann & al. 1999). Considering these data an attempt was made to elaborate the seasonal plankton dynamics on the shelf. However, the results supported the suspicion that these data may have been over-interpreted because shelves are generally subjected to significant temporal and spatial variability (Barber & Smith 1981; Walsh 1991; Biscaye & Andersson 1994; Pilskaln & al. 1996). The question arises how representative a data set based on one monthly cruise is for the understanding of seasonal plankton dynamics of the north Norwegian shelf.

An additional uncertainty arising from the investigation at Nordvestbanken with its relatively simple topography is how representative this bank area is for the north Norwegian shelf in general. A continuous shelf does not exist in northern Norway because deep fjords penetrate the shelf to the shelf edge, creating a series of coastal banks. What phytoplankton variability can be expected on a daily or weekly time scale and what differences in phytoplankton biomass are there to be found at the shelf break, on coastal banks and fjordic depressions between these banks? These questions can only be addressed if a polygon covering the entire shelf between coastal banks

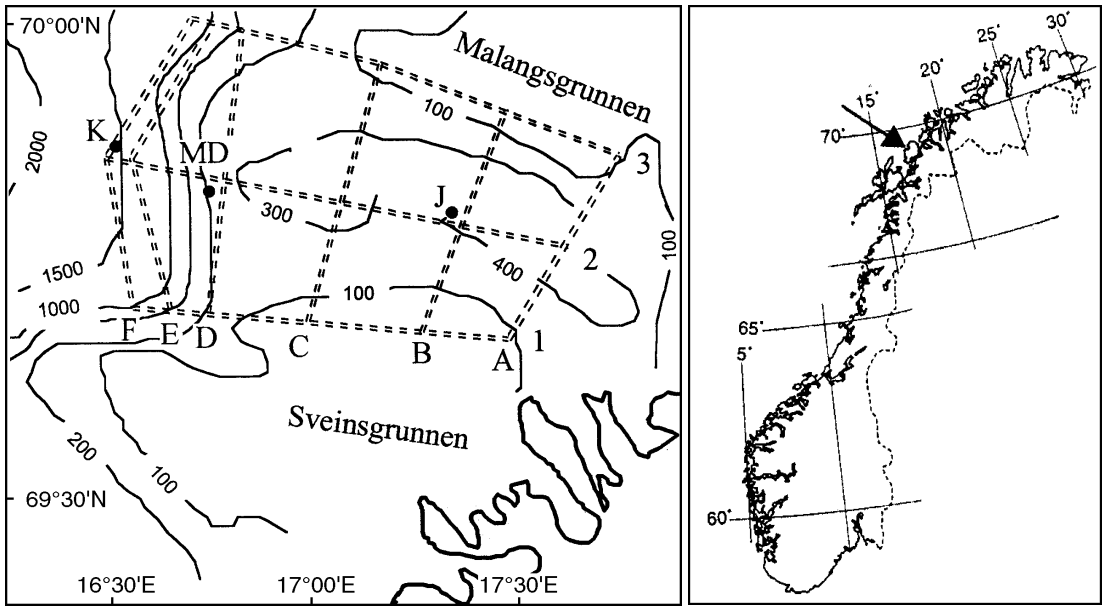

Fig. 1. The study area, ship tracks and sampling stations. The polygon was covered once in May and twice in June and September 1995. The lidar data were collected in along track measurements between stations A1 and E3. At the stations the water sampling and CTD measurements were performed, and the lidar was switched from integration to stratification mode. Also shown are stations from previous investigations: M.D. in 1991-1993 (Hegseth & al. 1995) and stations J and K from 1994 (P. Wassmann & I.J. Andreassen, unpubl. res.).

can be investigated during relatively short time intervals and the sampling frequency is detailed enough to create a basis to investigate the question of small temporal and spatial scales. In order to achieve this goal a remote sensing technique (lidar) was selected to investigate phytoplankton biomass as reflected by chlorophyll *a* (Chl *a*). Conventional sampling was kept to a minimum in order to save cruising time.

The laser remote sensing (lidar) technique has been widely applied in marine investigations over the last decades (Hoge & Swift 1981; Reuter & al. 1993; Babichenko & al. 1995). The prospects of its implementation into biomonitoring are defined by the capability of obtaining extensive information with high spatial resolution from large sea surface areas. One of the principal merits of laser remote sensing is relative independence of the measurements on external conditions like sunlight illumination, weather, water transparency and state of water surface.

In laser remote sensing *in vivo* Chl *a* fluorescence at the monochromatic excitation serves as an indicator of phytoplankton abundance in water. The integral fluorescence intensity of Chl *a* normalised by the integral intensity of Raman scattering of laser emission in water, called the fluorescent factor Φ, is usually interpreted as a measure of Chl *a* abundance (Bristow & al. 1981). The method of selective excitation of phytoplankton pigments was used to analyse mixed phytoplankton communities (Babichenko & al. 1993). The pump-and-probe technique can also be applied to estimate the primary photosynthetic processes (Chekaljuk & Gorbunov 1994). The ratio of Φ and Chl *a* concentration depends on the pigments of phytoplankton cells (taxonomic composition) as well as on the physiological stage of phytoplankton community (Poryvkina & al. 1994).

The present investigation is part of the project "Comparative fluxes of biogenic matter and trophodynamic interactions across the shelf break of northern Norway". The project in turn is a segment of the Ocean Margin EXchange programme (OMEX) which takes into account the specific features of the European shelves. OMEX concerns essentially the study of fluxes and processes occurring along European shelf break facing the North Atlantic Ocean. Its aim is to measure and model exchange processes at the ocean margin as a basis for the development of global models to predict the impact of environmental changes on the oceanic system and more specifically on the coastal zone.

Extensive variation in ocean climate influences the plankton dynamics of the north Norwegian coastal zone (Sundby 1984; Wassmann & al. 1996) and the adjacent Barents Sea (Midttun & Loeng 1987; Slagstad & Wassmann 1997). Based on the current understanding of the physical oceanography of the area (Sætre & Mork 1981; Sundby 1984; Moseidjord & al. 1999; Nordby &

al. 1999) profound seasonal effects on the dynamics of nutrients and phytoplankton over the shelf and the shelf break of northern Norway were expected, similar to those reported previously (Rey 1981; Peinert & al. 1986; Hegseth & al. 1995; Ratkova & al. 1999; Wassmann & al. 1999). Here we investigated the small-scale spatial variability and few-days' dynamics of phytoplankton biomass on a north Norwegian shelf area that includes a shelf break, coastal banks and a fjordic depression between the banks. We compared the results with previous investigations in the area.

MATERIAL AND METHODS

Three cruises of 6 days' duration each on board of R/V *Jan Mayen* were planned in May, June and September 1995 on a polygon with co-ordinates 69°40'-70°00'N, 16°30'-17°47'E. This polygon (Fig. 1) is situated on the shelf outside northern Norway (Malangsdjupet). Malangsdjupet is a continuation of the fjord Malangen between the two coastal banks Sveinsgrunnen and Malangsgrunnen. The average depth of Malangsdjupet is about 200 m while the banks are less than 100 m deep. The shelf break is situated about 40 nautical miles west of the outer coastline. Here, depth decreases sharply down to 1000 m and more. The flow of the Norwegian Coastal Current (NCC) and the North Atlantic Current (NAC) over the shelf and along the shelf break, respectively, gives rise to partial and variable intrusion of different water masses into Malangsdjupet. There is an inflow along the southern and an outflow along northern slope of the trench. Crossover from the southern to the northern side is probable throughout Malangsdjupet. In the centre inner part water from the fjord Malangen adds to the surface coastal water leaving Malangsdjupet on its northern side. The hydrophysical structure and dynamics of the studied area are thus influenced by interactions of Atlantic water and coastal waters as well as by the topography of the Malangsdjupet area.

The 6 transects A-F of the polygon were investigated consecutively and each sampling period for the 6 transects had a duration of about 18 hours. Samples were taken at 10 depths ranging from 0 to 100-150 m at 3 stations on all of the 6 polygon transects (A1-A3, B1-B3 etc., see Fig. 1). The distance between the stations was about 10-15 nautical miles. During each cruise the 6 transect runs were planned to be carried out every second day, i.e. 3 times per cruise. Because of a mechanical failure during the cruise in May and bad weather in both June and September, the transects could only be investigated once in May and twice in June and September.

Standard hydrographic sampling was carried out with a Neil Brown Mk III CTD-profiler mounted with a General Oceanic Rosette Sampler equipped with 5-litre Niskin bottles at each of the 15 stations. Samples for nutrients and suspended chlorophyll *a* were taken. Nutrient samples for nitrate, silicate, and phosphate were handled and analysed by a Technicon autoanalyzer as described by Wassmann (1991) at the Institute of Marine Research, Bergen. Chl *a* was measured with a Turner Designs AU-10 fluorometer. 250-500 ml from each depth were filtered through a 25 mm Whatman GF/F glass fibre filter. The filters were extracted with 10 ml of methanol for 2 hours at room temperature in the dark (Holm-Hansen & Riemann 1978). The samples were analysed according to Holm-Hansen & al. (1965). Calibration of the fluorometer was carried out with pure chlorophyll *a* from SIGMA Chemical Co.

The remote sensing was carried out by means of the Fluorescent Lidar System FLS-S. The remote laser spectrometer (lidar) is based on two lasers. The first one (XeCl excimer laser ELI-131, emission wavelength 308 nm, pulse energy 90 mJ, pulse duration 30 ns) pumps the second one, a tuneable dye-laser (DL-Lidar). The dye-laser generates light in the visible spectral range. The efficiency of energy transformation from UV to the visible spectral range is up to 15 %. By tuning the dye-laser, the wavelength of sensing emission can be selected in a range of excitation spectra of different phytoplankton pigments. Laser induced fluorescence and scattering are collected by a receiving telescope (light aperture 180 mm, focal distance 650 mm) with integrated spectral unit. It consists of a flat field polychromator with concave diffraction grating (450 l/mm) and input glass optical filter. The non-slit optical scheme of the polychromator is used to minimise the loss of energy. The output spectrum has a width of 300 nm and a spectral resolution of 1.5 nm. The intensified liner CCD camera (512 channels) serves as optical detector. By synchronising with laser pulse it registers the total spectral distribution of fluorescence and scattering in one read-out cycle (10 ms). The gated mode of the detector was used to localise the sensing volume in the water as well as to eliminate the sun light influence. The amplitude of the strobe pulse influences the sensitivity of the detector, its delay to the laser pulse gives the possibility to change the depth of sensing and the width of strobe defines the length of sensed water column. All parameters of the lidar are changed by software, providing flexibility of operational using. To estimate the concentration of Chl *a* by laser remote sensing, a preliminary calibration of the lidar was performed in the laboratory by using pure phytoplankton cultures.

In the present experiment the lidar FLS-S was installed on the open deck of R/V *Jan Mayen*. The sensing was carried out via a rotating mirror, which deflected the laser beam to the water area uninfluenced by the ship movement. The distance to the water surface was about 15 m. In general the ship kept a constant speed of about 4 knots

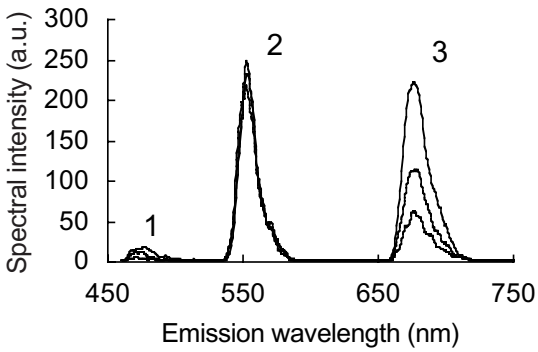

Fig. 2. The typical spectra of the north Norwegian shelf water at the laser excitation 460 nm. 1: Relay scattering suppressed by optical filter; 2: Raman scattering; 3: Chl *a* fluorescence.

between each of the contact sampling stations. In along-track measurements the lidar was adjusted to integrate the signals in water column from 5 m to 30 m. The receiving telescope was focused under the water to eliminate the influence of waves during stormy weather conditions. The underway sensing was performed along the tracks of 20-30 nautical miles with horizontal spatial resolution of 100-150 m, depending on the vessel speed. In stratification measurements at the contact sampling stations the lidar consistently sensed the water layers and shifted the sensing depth with a step interval of 3 m.

During the first cruise different sensing wavelengths were tested for direct excitation of Chl *a* (440 nm), excitation of combinations Chl *a* and Chl *c* (460 nm), Chl *a* and Chl *b* (480 nm) and Phycoerythrin (525 nm). The wavelength of 460 nm was selected as operational one due to homogeneous pigment structure of phytoplankton community, as reflected by the lidar. It fits to the excitation band of *in vivo* Chl *a* fluorescence and at the same time the phaeopigments are not excited as effectively as at the wavelength of 440 nm.

The typical spectral distribution of secondary emission contains three types of signals which are interpreted (Fig. 2). The first one is the Relay scattering line caused by elastic scattering of laser emission in a water column. The second spectral line is caused by Raman (inelastic) scattering on water molecules. The last one is used as normalising value for Chl *a* fluorescence to produce the fluorescent factor Φ. In a result the fluorescent factor itself does not depend on the conditions of measurement (sunlight illumination, weather, water transparency, and state of water surface). The fluorescence band of Chl *a* has a maximum at the wavelength of 680 nm. When the ship was travelling, the remote sensing spectra were registered for each laser pulse, with the following processing of the fluorescent factor Φ and storage of data. As the spectral signal/noise ratio per single laser pulse was at the level 10, the spectra were integrated over 10 laser pulses to increase the signal/noise ratio up to 30. Finally the accuracy of the Φ value determination was higher than 0.1. The number of sensing spots in each route over the polygon corresponded to 100 000 sampling procedures.

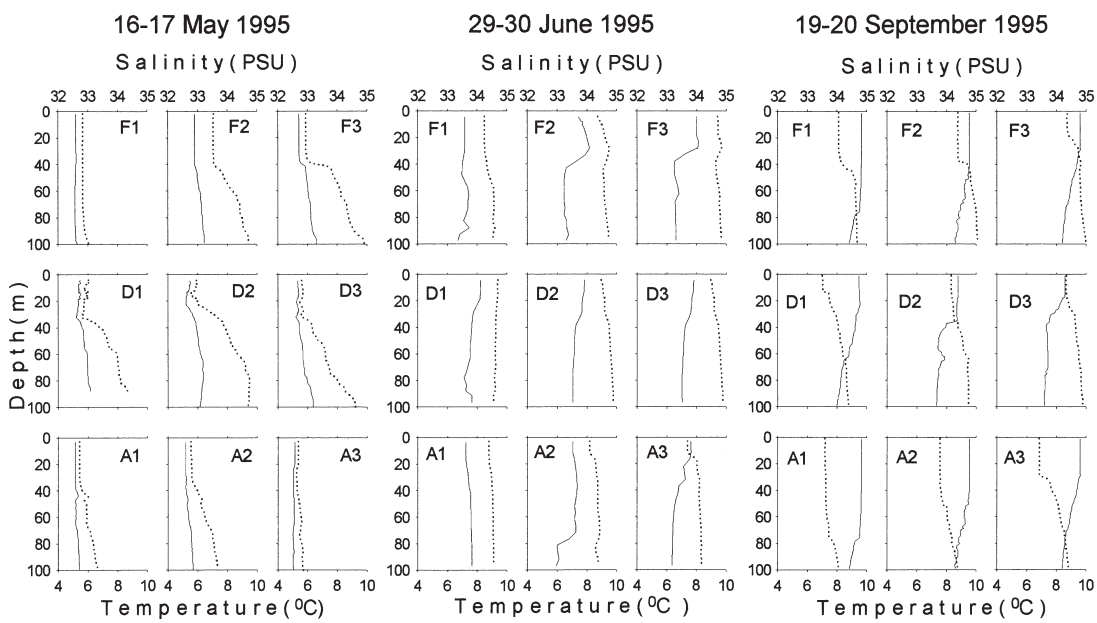

Fig. 3. The vertical profiles of the temperature (solid lines) and salinity (dotted lines) at the stations of the tracks A, D and F during one run in May, June, and September 1995.

RESULTS

Fig. 3 illustrates the variations of the temperature and salinity in the study area during the three cruises. The vertical profiles of salinity and temperature indicated significant temporal and spatial variability. In May the surface water was less saline at all stations in comparison with other two cruises. There was an obvious difference in salinity profiles at the depth more than 40 m between the stations. The salinity and temperature generally increased with the depth. At the same time more saline water was dominated at the transect D and at Stns F2 and F3 (Fig.3). In June the situation was different as both temperature and salinity did not indicate much variability throughout the polygon. More saline water was observed at all stations with relatively constant distribution in the depth. The temperature profiles tended to decrease with the depth. Expressed bounces of the temperature at the depth of 40 m were recorder at the Stns F2 and F3. In September the salinity of surface water was higher than in May and similar to the data recorded in June. The difference between the southern and northern side of the polygon was revealed. Less saline water was detected along the southern side of the entire polygon (Fig. 3: A1, D1, and F1). More saline water was recorded deeper than 30 m at Stn A3 and throughout the water column at Stns D3 and F3 (northern side). The temperature was generally higher than in May and June and decreases smoothly with the depth.

Because of the interaction between Atlantic and coastal waters the salinity is generally higher near the shelf break during all seasons (compare data from the stations F1-F3 and A1-A3). There is also a tendency of clearly increased salinity with increasing depth in the area of Atlantic water intrusion over the shelf break. The general picture of temperature and salinity variability shows that the eddy and possibly frontal structures present in the polygon.

As the depth of light penetration (euphotic zone) influences the phytoplankton distribution, the investigations of optical properties of the water in the study area were carried out. The water transparency was calculated as a characteristic depth of the exponential decay of Raman signal with the depth when the lidar was set in stratification mode at the sampling stations. Fig. 4 shows the map of water transparency in the study area. The data obtained show that the polygon can be conditionally divided into three areas of different water transparency. Track A is situated in the area of lowest transparency (area 1, coastal waters; characteristic depth is 18 m on average). The area 2 with medium transparency (22 m on average) is exemplified by tracks B and C. The maximal transparency (characteristic depth is up to 27 m) was recorded at the tracks D-F (area 3, near the shelf break).

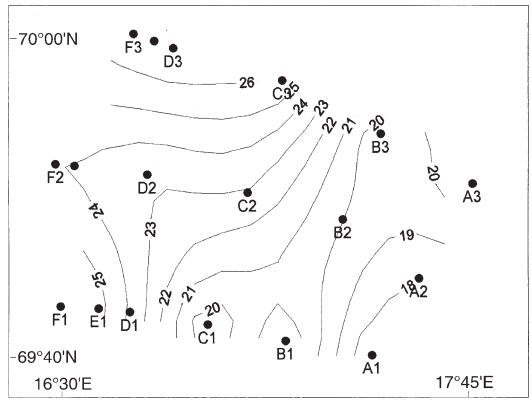

Fig. 4. Characteristic depths (m) of light penetration at the wavelength of 460 nm in the study area during May 1995.

The structure of optical properties corresponds to the hydrophysical conditions of water mixing caused by the interaction of more transparent Atlantic water across the shelf break and less transparent coastal water closer to the coast line and out of adjacent fjords.

Fig. 5 presents the results of the along-track abundance of phytoplankton biomass at selected runs. The measured tracks are aligned in South - North direction (see Fig.1 for tracks' location). In May and June significant patchiness was recorded. In September the Chl *a* concentrations were more evenly distributed. Besides the seasonal differences, the analysis of phytoplankton data revealed some common distribution features in the polygon. The mean concentrations of phytoplankton along the tracks B and C were lower than corresponding values in coastal waters (track A) and near the shelf break (tracks E-F) in all series of measurements. There were more obvious horizontal structures of phytoplankton distribution in the coastal zone in May and June (tracks A-C) as compared to other areas of the polygon. The vertical profiles of Chl *a* measured in water samples at the stations were more or less uniform and did not reveal expressed stratification at depths up to 100 m (data not shown).

The highest Chl *a* concentrations were observed in May. The measurements were carried out in smooth weather conditions. The phytoplankton distribution had a distinct patchy structure in the areas 1 and 2 (Fig. 5, tracks A-C). The typical scale of spatial variability was about 1.5-2.5 nautical miles. The conspicuous patch of phytoplankton between stations A2 and A3 was also found in tracks B and C. The phytoplankton concentration in the areas 1 and 2 had a positive trend when moving to the north of the polygon while in track D the maximum concentration shifted to the south.

The weather conditions were different in the two runs in June. The second run (dotted line at the Fig. 5) was

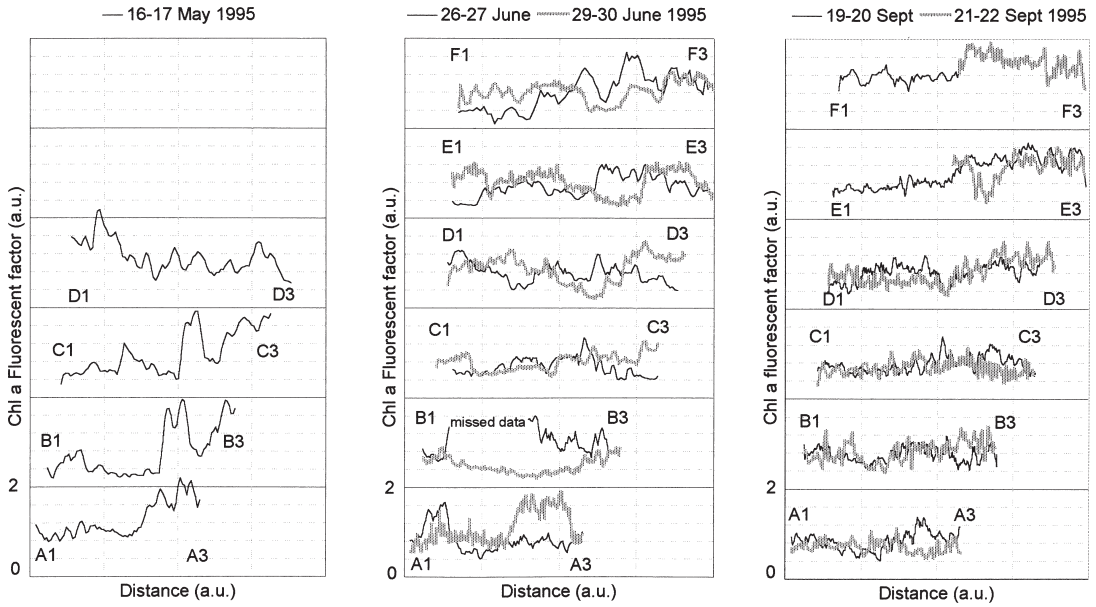

Fig. 5. Integrated Chl *a* abundance in the upper layers measured by the lidar along the transects expressed by fluorescent factor.

performed after a storm. Chl *a* concentrations were similar as compared to the first run (solid line) on the southern part of the polygon in area 1 (Fig. 5, June, track A). A maximum appeared during the second run at the northern part of track A. The spatial distribution of phytoplankton in area 2 (Fig. 5, June, track C) was more homogeneous in the second run when comparing with the previous one. On the track B, however, large differences were recorded in the mid track section. Some periodical structures were recorded in area 3 during the first run. However, after the storm the Chl *a* distribution was more smooth in area 3 (Fig. 5, June, tracks D-F).

The general level of phytoplankton concentration in September was slightly higher in area 2 and 3 compared to June. Conspicuous patches of Chl *a* were not detected. The difference of phytoplankton distribution in the different areas was small. At the same time the maximum abundance of phytoplankton was observed in the northwestern part of the polygon (Fig. 5, September, tracks D-E). This was not typical for the previous seasons. The data of the second run were similar to the first one. The weather conditions on both runs were relatively rough.

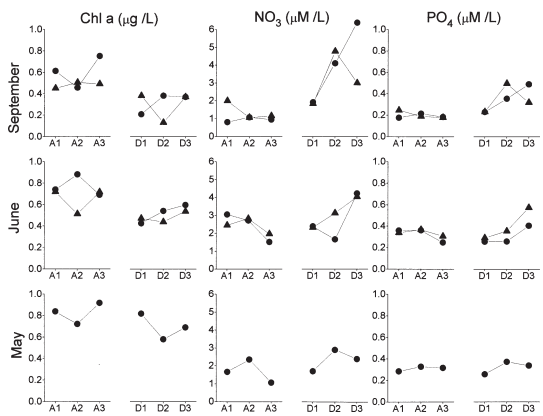

Fig. 6. Variability of contact Chl *a* (μg L^{-1}) and nutrients (μM L^{-1}) at the stations of tracks A and D. Circles: first run; triangles: second run. The data are averaged through the 0-50 m depth interval.

In order to detect the spatial and temporal variability in sampling data, the concentrations of phytoplankton and nutrients were averaged over the upper 50 m of the water column (Fig. 6). The correlation between Chl *a* and nutrients at the stations was typically negative (Fig. 6) which implies that patches of water at different successional stages pass through the polygon. The nutrient concentrations at Stns D2 and D3 were often higher compared to Stn D1 and A1-A3. This reflects an uplift of nutrient-rich water over the outer edge of Sveinsgrunnen when water from Malangsdjupet joins the NAC with its high current speed along the shelf break. The correspondence of remote and contact data at the sampling stations in all seasons was also investigated (Fig. 7). The Chl *a* values obtained by conventional and remote measurements were well correlated ($r^2 = 0.74$, n = 61). Thus the regression line can be used to calibrate remote sensing data.

Fig. 8 presents an example of the variation of Chl *a* horizontal distribution in comparison with vertical profiles of temperature and salinity in three days interval.

Results from track A (Stns A1-A3) in June were selected. During the first run the maximum phytoplankton biomass was detected near Stn A1, while it had disappeared along the second run (three days later). A new patch of increased phytoplankton biomass was recorded between Stns A2 and A3 during the second run. The vertical profiles of temperature at Stn A1-A3 were quite different for the first and second track while changes in salinity were less obvious. The differences could have been caused by the dynamics of coastal water, supporting the assumption that differences in spatial structures of phytoplankton biomass may be influenced by hydrophysical conditions. However, a careful investigation of Fig. 8 reveals that the profiles of the temperature and salinity in water transporting a patch of Chl *a* on 26 June (Stn A1) in the south are quite different from those of the patch observed in the north on 29 June (Stn A3). Obviously, these were two different bodies of water which have increased phytoplankton biomass in common.

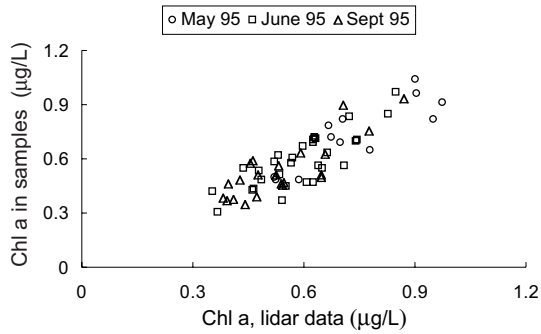

Fig. 7. Correlation between remote and contact Chl *a* estimates at the sampling stations during all runs and seasons.

DISCUSSION

The hydrodynamic and concomitant phytoplankton biomass scenarios encountered across the Malangsdjupet polygon were subjected to significant variability over periods of time which are far shorter than revealed by traditional sampling. This implies that previous hydrographic and plankton data could have been misinterpreted as they were discussed as characteristic for the sampling frequency, i.e. at the best on a weekly, but very often on a monthly scale (e.g. Rey 1981; Evensen 1994; Hegseth & al. 1995; Wassmann & al. 1999). The present data obtained by laser remote sensing revealed high spatial and temporal dynamics of phytoplankton biomass on the north Norwegian shelf (Figs 5 & 8). This variability could only to a much lesser extent be detected by conventional contact sampling procedures (Fig. 6). The typical spatial scales of phytoplankton distribution in calm weather conditions corresponded to 1.5-2.5 nautical miles in May and June. The vertical profiles of contact phytoplankton biomass revealed a relatively uniform distribution.

The combination of several factors can be responsible

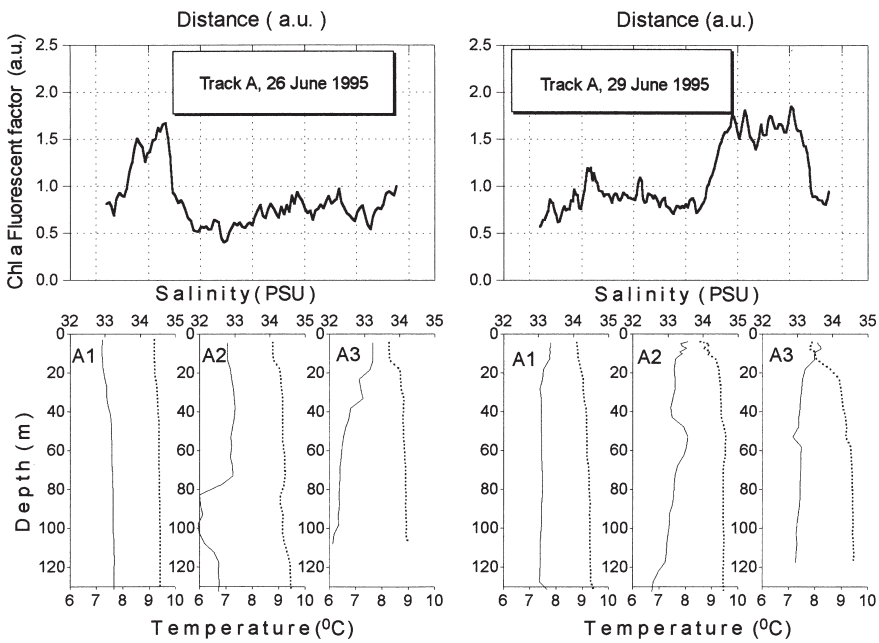

Fig. 8. Short time variability of Chl *a* distribution and temperature and salinity along track A on 26 and 29 June.

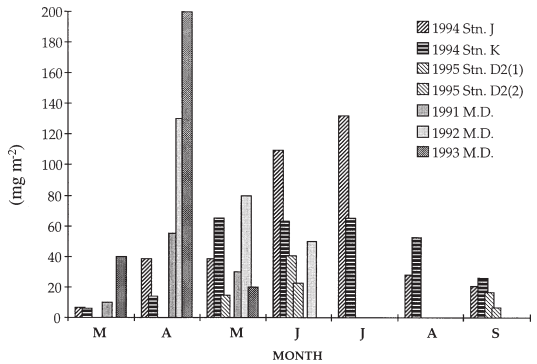

Fig. 9. Seasonal variation of integrated contact Chl *a* concentrations in the upper 50 m from the Malangsdjup station (M.D.) in 1991-1993 (Hegseth & al. 1995), station J and K in 1994 (P. Wassmann, unpubl. res.) and C2 and F2 (this study). See Fig. 1 for positions.

for the spatial and temporal variability of the phytoplankton distribution. Internal waves can induce the surface fluctuations in the direction of wave phase propagation. This may lead to the grouping of passive ingredients, including phytoplankton into well-expressed structures. As the internal Rossby radius in the study area is approximately 4 km, the cyclonic and anticyclonic eddies would tend to have similar dimensions. The spatial structures of phytoplankton distribution detected in a smooth weather were similar to this scale (see Fig. 5, May and first run in June). The topography can have some influence especially adjacent to fjords which can enhance formation of eddies and following phytoplankton structures. As described above, the features of spatial distribution of phytoplankton were different near the shelf break (tracks D-F), in the central part of the polygon (tracks B and C), and near the coastal zone (track A). The weather conditions can play an additional role as the wind provides the variations in energy input. It is supported by the fact that during a storm weather the spatial distribution of phytoplankton biomass was more smooth, and spatial structures, when detected, had smaller scales (Fig. 5, second run in June, both runs September).

The measured phytoplankton distributions seem to indicate that patches are quite dynamic and may appear in the polygon in a scale of a few days. In order to investigate the seasonal and spatial variability in the Malangsdjup area in sufficient detail the optimal temporal scale should be a few days and the optimal spatial scale less then few nautical miles. Obviously, such an investigation would be far too demanding to be realistic in the frame of current investigation schedules.

Given the complexity and the hydrodynamic variations of the north Norwegian shelf (Sundby 1984; Nordby & al. 1999), the question can be raised to what extent a number of measurements on nutrients and suspended matter at a given date and site are representative for more then a scale of a day and some m^3. Assuming a horizontal displacement of surface water of 10-20 cm s^{-1} along the shelf break (tracks E and F) and in a circular pattern through Malangsdjupet along the edge of Sveinsgrunnen and Malangsgrunnen (tracks A-D), the residence time inside the polygon can be approximated (Moseidjord & al. 1999). According to these calculations a patch of phytoplankton biomass would need 2-4 days to pass through the polygon along the shelf break (F1-F3). A full circle throughout Malangsdjupet would take 6-12 days, from B1 to B3 about 2-4 days. This simple calculation exemplifies the basic problem of interpreting plankton data from dynamic shelf regions: over a short period of time the nutrients and plankton may differ remarkably. Across the north Norwegian shelf and in various depth intervals the residence time and current direction can clearly change. While the current along the shelf break is strong and more or less unidirectional, anticyclonic water movement and variable residence times are observed on the banks (Sundby 1984; Orvik 1995). In the trenches between the banks, however, the general water movement is cyclonic, but topography strongly influences this pattern. In addition, the tide modifies these current and residence time patterns (Nordby & al. 1999). These hydrodynamic and pelagic features are probably not specific for the north Norwegian shelf, but valid for many hydrodynamic active shelves of non-upwelling regions.

A comparison of Chl *a* concentrations from several investigations in the polygon area revealed a conspicuous variability (Fig. 9). No clear seasonal trend of the vernal bloom was observed as maxima were recorded in April, June and as late as July. The Chl *a* concentrations ranged by a factor of 2-16 for the months March-September, with an average of about 6. The concentrations at Stns J and A2 which were more remote from the shelf break compared to Stns K and D2 had most of the time higher Chl *a* concentrations (see Fig. 1). Similar trends have previously been recorded on the north Norwegian shelf by Rey (1981) and Wassmann & al. (1999). These differences have been interpreted as the consequence of increasing grazing along gradients from fjords towards the shelf break (Ratkova & al. 1999). This also seems reflected in the highest Chl *a* concentrations (about 200 mg Chl *a* m^{-2}) which were observed at the M.D. station in 1993 (Hegseth & al. 1995), a year when the meso-zooplankton biomass in the area was low (T. Falkenhaug, pers. commn). In 1994 and 1995 when meso-zooplankton biomass was higher (E. Nordby & K.S. Tande, pers. commn) and the Chl *a* concentrations were accordingly lower. Fig. 9 illustrates clearly that the spatial, seasonal and inter-annual variability in phytoplankton biomass on the north Norwegian shelf is substantial.

Care must be taken to interpret seasonal or spatial phytoplankton distribution on the north Norwegian shelf when sampling is carried out at time intervals greater then 1 day and the spatial resolution is less then a few nautical miles. The application of laser remote sensing techniques in regular bio-monitoring of natural waters opens the door to (a) rapid and detailed quantification of phytoplankton abundance and (b) optimise the number of conventional sampling procedures.

ACKNOWLEDGEMENTS

The authors thank Sigrid Øygarden for support in the laboratory and the officers and crew of the R/V *Jan Mayen*. Jane Strømstad analysed the nutrient samples. The authors thank Dr. Jüri Elken for useful discussions. This work was supported by the Research Council of Norway (project no. 101323/410 and 108085/122) and the European Union in the framework of the MAST programme, contract no. MAS2-CT93-0069 and MAS3-CT96-0056 (Ocean Margin EXchange - OMEX).

REFERENCES

Babichenko S, Kaitala S, Poryvkina L. 1995. Multiple-wavelength remote sensing of phytoplankton. *EARSeL Journal Advances in Remote Sensing* 3:78-83.

Babichenko S, Poryvkina L, Arikese V, Kaitala S, Kuosa H. 1993. Remote sensing of phytoplankton using laser induced fluorescence. *Remote Sensing of Environment* 45:43-50.

Barber RT, Smith WO. 1981. Coastal upwelling ecosystems. In: Longhurst AR, editor. *Analysis of marine ecosystems.* New York: Academic Press. p 31-68.

Biscaye PE, Anderson RF. 1994. Fluxes of particulate matter on the slope of the southern mid-Atlantic Bight. *Deep-Sea Research* 4:459-509.

Bristow M, Nielson D, Bundy D, Furtek F. 1981. Use of water Raman emission to correct airborne laser fluorescence sensor data for effects of water optical attenuation. *Applied Optics* 20:2889-2906.

Chekaljuk A, Gorbunov M. 1994. Pump-and-probe lidar fluorosensor and its applications for estimates of phytoplankton photosynthetic activity. In: *Proceedings of Second Thematic Conference Remote Sensing for Marine and Coastal Environments*; New Orleans, USA. 1:381-400.

Evensen A. 1994. *Planteplankton i Barentshavet: Artssammensetning og suksesjon. Regionale variasjoner i vår-oppblomstringen relatert til miljø* [Cand.scient. thesis]. Tromsø, Norway: University of Tromsø. 137 p.

Fernandez E, Cabal J, Acuna JL, Bode A, Botas A, Garcia-Soto CG. 1993. Plankton distribution across a slope current-induced front in the southern Bay of Biscay. *Journal of Plankton Research* 15:619-641.

Hegseth EN, Svendsen H, Quillfeldt CH von. 1995. Phytoplankton in fjords and coastal waters of northern Norway: environmental conditions and dynamics of the spring bloom. In: Skjoldal HR, Hopkins C, Erikstad KE, Leinaas HP, editors. *Ecology of Fjords and Coastal Waters*. Amsterdam: Elsevier Science. p 45-72.

Hoge FE, Swift RN. 1981. Airborne simultaneous spectroscopic detection of laser-induced water Raman backscatter and fluorescence of chlorophyll a and other naturally occurring pigments. *Applied Optics* 20:3197-3205.

Holligan PM, Williams PJ leB, Purdie D, Harris RP. 1984. Photosynthesis, respiration and nitrogen supply of plankton populations in stratified, frontal and tidally mixed shelf waters. *Marine Ecology Progress Series* 17:201-213.

Holm-Hansen O, Lorenzen CJ, Holmes RW, Strickland JDH. 1965. Fluorometric determination of chlorophyll. *Journal du Conseil International pour l'Exploration de la Mer* 30:3-15.

Holm-Hansen O, Riemann B. 1978. Chlorophyll determination: improvement of the in methodology. *Oikos* 30:3-15.

Kahru M, Elken J, Kotta I, Simm M, Vilbaste K. 1984. Plankton distributions and processes across a front in the open Baltic Sea. *Marine Ecology Progress Series* 20:101-111.

Kiørboe T, Munk P, Richardson K, Christensen V, Paulsen H. 1988. Plankton dynamics and larval herring growth, drift and survival in a frontal area. *Marine Ecology Progress Series* 44:205-219.

Legendre L, Le Fèvre J. 1989. Hydrodynamical singularities controls of recycled versus export production in oceans. In: Berger WH, Smetacek V, Wefer G, editors. *Productivity of the Ocean: Present and Past*. Chichester: Wiley & Sons. p 49-63.

Legendre L, Le Fèvre J. 1995. Microbial food webs and the export of biogenic carbon in the ocean. *Aquatic Microbial Ecology* 9:69-77.

Midttun L, Loeng H. 1987. Climatic variations in the Barents Sea. In: Loeng H, editor. *The effect of oceanographic conditions on distribution and population dynamics of commercial fish stocks in the Barents Sea.* Proceedings 3rd Soviet-Norwegian Symposium; Institute of Marine Research, Bergen, Norway. p 13-27.

Moseidjord H, Slagstad D, Svendsen H. 1999. Sensitivity studies of circulation and ocean-shelf exchange off northern Norway. *Sarsia* 84:191-198.

Nordby E, Tande KS, Svendsen H, Slagstad D. 1999. Oceanography and fluorescence at the shelf break off the north Norwegian coast (69°20'N-70°30'N) during the main productive period in 1994. *Sarsia* 84:175-189.

Orvik KA. 1995. Topographic influence on the flow field off Lofoten Vesterålen. In: Skjoldal HR, Hopkins C, Erikstad KE, Leinaas HP, editors. *Ecology of Fjords and Coastal Waters.* Amsterdam: Elsevier Science. p 165-175.

Peinert R. 1986. Production, grazing and sedimentation in the Norwegian Coastal Current. In: Skreslet S, editor. *The role of freshwater outflow in coastal marine ecosystems.* NATO ASI Series, Vol G7. Berlin: Springer Verlag. p 361-374.

Pilskaln CH, Paduan JB, Chavez FP, Andersson RY, Berelsen WM. 1996. Carbon and regeneration in the coastal upwelling system of Monterey Bay, central California. *Journal of Marine Research* 54:1149-1178.

Poryvkina L, Babichenko S, Kaitala S, Kuosa H, Shalapjonok A. 1994. Spectral fluorescence signatures in characterisation of phytoplankton community composition. *Journal of Plankton Research* 16:1315-1327.

Ratkova N, Wassmann P, Verity PG, Andreassen IJ. 1999. Abundance and biomass of pico-, nano-, and microplankton on a transect across Nordvestbanken, north Norwegian shelf, in 1994. *Sarsia* 84:213-225.

Reuter R, Diebel D, Hengstermann T. 1993. Oceanographic laser remote sensing: measurement of hydrographic fronts in the German Bight and in the Northern Adriatic Sea. *International Journal of Remote Sensing* 14:823-848.

Rey F. 1981. Primary production estimates in the Norwegian Coastal Current between 62°N and 72°N. In: Sætre R, Mork M, editors. *The Norwegian Coastal Current*. University of Bergen. p 640-648.

Sætre R, Mork M. 1981. *The Norwegian Coastal Current*. University of Bergen. 795 p.

Slagstad D, Wassmann P. 1997. Climate change and carbon flux in the Barents Sea: 3-D simulations of ice-distribution, primary production and vertical export of particulate organic matter. *Memoirs National Institute of Polar Research, Special Issue* 51:119-141.

Sundby S. 1984. Influence of bottom topography on the circulation at the continental shelf of northern Norway. *Fiskeridirektoratets Skrifter Serie Havundersøkelser* 17:501-519.

Walsh JJ. 1991. Importance of continental margins in the marine biogeochemical cycling of carbon and nitrogen. *Nature* 350:53-55.

Wassmann P. 1991. Sampling and analysis of marine particles with PEBENOCO (Pelagic-Benthic Coupling in the Norwegian Coastal Zone), University of Tromsø, Norway. In: Hurd DC, Spencer DW, editors. *Marine Particles: Analysis and Characterization*. Geophysical Monograph 63. p 97-99.

Wassmann P, Andreassen IJ, Rey F. 1999. Seasonal variation of nutrients and suspended biomass on a transect across Nordvestbanken, north Norwegian shelf, in 1994. *Sarsia* 84:199-212.

Wassmann P, Svendsen H, Keck A, Reigstad M. 1996. Selected aspects of the physical oceanography and particle fluxes in fjords of northern Norway. *Journal of Marine Systems* 8:53-71.

Accepted 17 December 1998 – Printed 15 November 1999
Editorial responsibility: Ulf Båmstedt